AIP | The Journal of Chemical Physics

Time-dependent wave packet calculation for state-to-state reaction of Cl+H 2 using the reactant-product decoupling approach

Yici Zhang, Jingfeng Zhang, Haiyan Zhang, Qinggang Zhang, and John Z. H. Zhang

Citation: The Journal of Chemical Physics **115**, 8455 (2001); doi: 10.1063/1.1388557
View online: http://dx.doi.org/10.1063/1.1388557
View Table of Contents: http://scitation.aip.org/content/aip/journal/jcp/115/18?ver=pdfcov
Published by the AIP Publishing

Time-dependent wave packet calculation for state-to-state reaction of Cl+H_2 using the reactant-product decoupling approach

Yici Zhang,[a] Jingfeng Zhang, Haiyan Zhang, and Qinggang Zhang
Department of Physics, Shandong Teachers' University, Jinan, Shandong, China

John Z. H. Zhang[b]
Department of Chemistry, New York University, New York, New York 10003

(Received 15 May 2001; accepted 8 June 2001)

We present in this paper the application of the reactant-product decoupling (RPD) method [T. Peng and J. Z. H. Zhang, J. Chem. Phys. **105**, 6072 (1996)] in a time-dependent wave packet calculation of the state-to-state reaction of $Cl+H_2 \rightarrow HCl+H$ on the G3 potential energy surface. In the RPD approach, the wave function is split into two components: the reactant ψ_R, which comprises the reagent and interaction regions, and the product ψ_P, which comprises the product region. The propagation of the reactant component ψ_R is separated (decoupled) from that of the product component ψ_P through the use of absorbing potential. The propagation ψ_P is entirely in the product space using the product Jacobi coordinates by using a coordinate transformation on the absorbed piece of wave function. The reaction probabilities from the ground state of H_2 to specific rovibrational states of the product ClH are presented in detail. All calculations are done for total angular momentum $J=0$ on the G3 potential energy surface. © *2001 American Institute of Physics.* [DOI: 10.1063/1.1388557]

I. INTRODUCTION

Currently, time-dependent wave packet (or more generally, initial value) methods provide efficient and practical ways to solve quantum dynamics problems for relatively large molecular systems. In a reactive scattering calculation, the application of time-dependent or equivalent methods is particularly convenient if one is only interested in total reaction probabilities or cross sections without the need to know specific product state distribution. This is because one can simply use the Jacobi coordinates corresponding to the entrance (or reactant) channel to propagate the wave packet. Significant progress has been made in the application of time-dependent methods to chemical reactions involving four[1,2] or more atoms.[3–5] In other words, the reactive scattering problem essentially becomes an inelastic scattering problem without the need for coordinate transformation between different arrangements. However, if final state-specific information is required such as in the calculation of product state distribution or differential cross section, the old ''coordinate problem'' again comes back to life. One straightforward approach is to simply switch the coordinates of the wave packet from the reactant to the product during the middle of the propagation while the wave packet is somewhere in the middle of the interaction region.[6,7] Although there is limited success to this switching approach, the method is generally unreliable because one could not control the wave packet—as it is localized in the interaction region—without spreading too much.

Recently, a reactant-product decoupling (RPD) method was proposed to tackle the ''coordinate problem'' for time-dependent wave packet calculation of state-to-state dynamics.[8–10] In the RPD approach, the complete wave packet is split into the reactant and product components. The resulting RPD equations are such that the propagation of the reactant wave packet is independent of that of the product components, and in addition each product wave packet can be propagated separately. Numerical test calculations have shown that the RPD approach can give accurate state-to-state S-matrix or reaction probabilities for atom–diatom reactions.[9,10] Theoretically, the RPD approach is exact regardless of how many partitionings one uses to split the wave packet. For example, one can further partition the wave packet into the reactant, interaction, and product components.[11–13] In addition, the location of the artificial potentials that separate the wave packet into different components can be chosen arbitrary. Recently, Althorpe fully explored this property by using a reflecting potential near the entrance region to maximize the computational efficiency and obtained excellent results of differential cross section for the $H+H_2$ reaction.[14]

So far the RPD approach has only been applied to the state-to-state calculation for the simplest $H+H_2$ and its isotopic reactions in reactive scattering.[9,10,14] A recent application of the RPD approach to photodissociation of water demonstrated that the RPD method is also an efficient approach to obtaining product state distribution in photofragmentation dynamics. In this paper, we apply the RPD method to calculate state-to-state reaction probability for the reaction $Cl(^2P)+H_2 \rightarrow HCl+H$. As shown in Ref. 8, the RPD scheme is quite general and can be implemented in both the time-dependent and energy-independent versions.[8] In the time-dependent version, the coordinate transformation is carried out at each time step, while in the energy-dependent version,

[a]Author to whom all correspondence should be addressed; electronic mail: yicizh@jn-public.sd.cninfo.net
[b]On leave at Department of Computational Science, National University of Singapore.

the coordinate transformation is carried out at every scattering energy of interest. For purpose of comparing with time-independent scattering calculations, we employed the G3 potential surface[15] in the present calculation.

This paper is organized as follows: Section II gives a brief review of the RPD approach and wave packet method for the $Cl+H_2$ reactive scattering. A more accurate version of the propagation equation for the product component wave function is also presented. Section III gives numerical results of the state-to-state reaction probabilities for the $Cl+H_2$ reaction with total angular momentum fixed at $J=0$. A comparison of state-to-state reaction probabilities with results from previous time-independent calculations is given. Section IV gives a summary of the present work and a discussion on future options to improve the accuracy of the RPD approach for state-to-state reactive scattering calculation.

II. THEORY

A. Reactant-product decoupling equations

The basic strategy of the RPD scheme is to partition the full TD wave function into a sum of reactant component (Ψ_r) and all product components [$\Psi_p(p=1,2,3,\ldots)$]

$$\Psi=\Psi_r+\sum_p \Psi_p \tag{1}$$

that satisfy the following *decoupled* equations:[8]

$$\begin{aligned} i\hbar\frac{\partial}{\partial t}|\Psi_r(t)\rangle &= H|\Psi_r(t)\rangle - i\sum_p V_p|\Psi_r(t)\rangle, \\ i\hbar\frac{\partial}{\partial t}|\Psi_p(t)\rangle &= H|\Psi_p(t)\rangle + iV_p|\Psi_r(t)\rangle, \end{aligned} \tag{2}$$

where H is the full Hamiltonian and $-iV_p$ is the generic ''absorbing'' potential. It is easy to verify that by adding all the above-mentioned equations together, one obtains the original Schrödinger equation for the full wave function Ψ—*independent* of the specific forms of the absorbing potential V_p. Of course, the behavior of the component wave functions will *depend* on the specific forms of the absorbing potential V_p. One can therefore choose the ''absorbing'' potentials and their locations to suit the specific situation on hand. For example, a recent work by Althorpe has shown that by cleverly employing a ''reflecting'' (real) potential near the entrance channel, the RPD approach can be made more efficient for state-to-state wave packet calculation.[14]

Equation (2) is *decoupled* in the sense that the solution for $\Psi_r(t)$ is independent of those for $\Psi_p(t)$ and the latter are independent of each other. If the absorbing potentials are perfect absorbers and are properly located in the regions after the point of no return, each component wave function should be the correct representation of the full wave function in their respective regions of space as shown in calculations of Refs. 9 and 10. When more complicated ''absorbing'' potentials are employed or they are located arbitrarily, a little more complicated analysis is required.[12,13]

Time-dependent wave packet calculation for Ψ_r can be efficiently carried out by using the Jacobi coordinates corresponding to the reactant arrangement, and the basic procedures of wave packet propagation are identical to those described in Ref. 16. The main difference in the present calculation for Ψ_r, however, is that we do not discard the absorbed piece of wave function $V_p\Psi_p(t)$ but instead store them in a proper representation on computer disk for later calculation of the product component(s) $\Psi_p(t)$ to be described later.

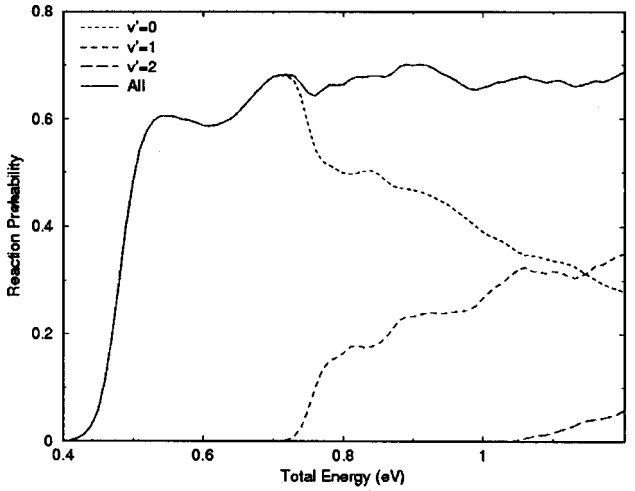

FIG. 1. Vibration-specific reaction probabilities for $Cl+H_2(00)\rightarrow ClH(v')+H$ where the product rotational states j' have been summed over. The total energy is the sum of ground rovibrational energy of H_2 and the translation energy.

For an atom–diatom reaction $A+BC$, there are two possible products (neglecting three body fragments): $B+AC$ and $C+AB$ as shown in Fig. 1. For a fixed total angular momentum J, the Hamiltonian of the system can be expressed in terms of the Jacobi coordinates of the reactant arrangement $A+BC$,

$$H=-\frac{\hbar^2}{2\mu_R}\frac{\partial^2}{\partial R^2}+\frac{(\mathbf{J}-\mathbf{j})^2}{2\mu_R R^2}+\frac{\mathbf{j}^2}{2\mu_r r^2}+V(\mathbf{r},\mathbf{R})+h(r), \tag{3}$$

where μ_R is the reduced mass between the center of mass of A and BC, $\mathbf{J}$ the total angular momentum operator of the system, $\mathbf{j}$ the rotational angular momentum operator of BC, and μ_r the reduced mass of BC. The diatomic reference Hamiltonian $h(r)$ is defined as

$$h(r)=-\frac{\hbar^2}{2\mu_r}\frac{\partial^2}{\partial r^2}+V_r(r), \tag{4}$$

where V_r is a diatomic reference potential (usually chosen as an asymptotic diatomic potential). The time-dependent wave function Ψ_r satisfying the absorbing boundary condition can be expanded in terms of the body-fixed translational–vibrational–rotational basis $\{u_n^v(R)\phi_v(r)Y_{jK}^{JM\epsilon}(\hat{R},\hat{r})\}$ as

$$\begin{aligned} &\Psi_{r,v_0 j_0 K_0}^{JM\epsilon}(\mathbf{R},\mathbf{r},t) \\ &\quad=\sum_{n,v,j,K} F_{nvjK,v_0 j_0 K_0}^{JM\epsilon}(t)u_n^v(R)\phi_v(r)Y_{jK}^{JM\epsilon}(\hat{R},\hat{r}), \end{aligned} \tag{5}$$

where n is the translational basis label, M is the projection quantum number of J on the space fixed z axis, (v_0,j_0,K_0)

denotes the initial rovibrational state, and ϵ is the parity of the system defined as $\epsilon=(-1)^{j+L}$ with L being the orbital angular momentum quantum number.

The functions $\phi_v(r)$ are eigenfunctions of the diatomic Hamiltonian of Eq. (4). The definition of the nondirect product basis functions $u_n^v(R)$ is given in Ref. 16. For the sake of clarity, we omit the labels $v_0 j_0 K_0$ and $JM\epsilon$ in the following discussion.

The split-operator propagation scheme for wave packet propagation is given as[17]

$$\Psi_r(\mathbf{R},\mathbf{r},t+\Delta)=e^{-iH_0\Delta/2}e^{-iU\Delta}e^{-iH_0\Delta/2}\Psi_r(\mathbf{R},\mathbf{r},t), \quad (6)$$

where the reference Hamiltonian H_0 is defined as

$$H_0=-\frac{\hbar^2}{2\mu_R}\frac{\partial^2}{\partial R^2}+h(r), \quad (7)$$

and the effective potential operator U in Eq. (6) is defined as

$$U=\frac{(\mathbf{J}-\mathbf{j})^2}{2\mu_R R^2}+\frac{\mathbf{j}^2}{2\mu_r r^2}+V(R,r,\theta)=V_{\rm rot}+V. \quad (8)$$

The matrix version of Eq. (6) for the expansion coefficient vector $\mathbf{F}$ is then given by

$$\mathbf{F}(t+\Delta)=e^{-i\mathbf{H}_0\Delta/2}e^{-i\mathbf{U}\Delta}e^{-i\mathbf{H}_0\Delta/2}\mathbf{F}(t) \quad (9)$$

and the operator $e^{-i\mathbf{U}\Delta}$ is further split as

$$e^{-i\mathbf{U}\Delta}=e^{-i\mathbf{V}_{\rm rot}\Delta}e^{-i\mathbf{V}\Delta}e^{-i\mathbf{V}_{\rm rot}\Delta} \quad (10)$$

where $V_{\rm rot}$ is diagonal in angular momentum basis representation and V is diagonal in coordinate representation.[16]

The initial wave function is chosen as the product of a specific rovibrational eigenfunction and a localized translational wave packet,

$$\Psi_i(0)=\varphi_{k_0}(R)\phi_{v_0 j_0}(r)Y_{j_0K_0}^{JM\epsilon}(\hat{R},\hat{r}), \quad (11)$$

where the wave packet $\varphi_{k_0}(R)$ is chosen to be a standard Gaussian function

$$\varphi_{k_0}(R)=\left(\frac{1}{\pi\delta^2}\right)^{1/4}\exp[-(R-R_0)^2/2\delta^2]e^{-ik_0R}. \quad (12)$$

The exact rovibrational function $\phi_{v_0 j_0}(r)$ of BC is expanded in terms of the reference vibrational functions $\phi_v(r)$ to generate the coefficient vector of the wave function at $t=0$.

B. Propagation of Ψ_p in the product arrangement

In the RPD method, one calculates the specific Ψ_p component wave function *independently* of other product components. In previous applications, the trapezoidal rule was used to propagate the Ψ_p. Here we derive a more accurate formula to propagate Ψ_p. The equation that determines Ψ_p in Eq. (2) has the formal solution

$$\Psi_p(t+\Delta)=e^{-(i/\hbar)H\Delta}\left[\Psi_p(t)+\frac{1}{\hbar}e^{-(i/\hbar)H\Delta}\times\int_t^{t+\Delta}e^{(i/\hbar)H(t'-t)}V_p\Psi_r(t')dt'\right]. \quad (13)$$

It is not difficult to show that the following relation holds:

$$-\frac{1}{\hbar}e^{-(i/\hbar)H\Delta}\int_t^{t+\Delta}e^{(i/\hbar)H(t'-t)}V_p\Psi_r(t')dt' =e^{(i/\hbar)H\Delta}\Psi_r(t+\Delta)-\Psi_r(t), \quad (14)$$

which gives the result

$$\Psi_p(t+\Delta)=e^{-(i/\hbar)H\Delta}[\Psi_p(t)+\Psi_r(t)-e^{(i/\hbar)H\Delta}\Psi_r(t+\Delta)] \quad (15)$$

$$=e^{-(i/\hbar)H\Delta}[\Psi_p(t)+(1-e^{(i/\hbar)H\Delta}e^{-(i/\hbar)(H-iV_p)\Delta})\Psi_r(t)]. \quad (16)$$

Since V_p is nonzero only in a small strip, we can make the approximation

$$e^{-(i/\hbar)(H-iV_p)\Delta}\approx e^{-(i/\hbar)H\Delta}e^{-(i/\hbar)V_p\Delta}, \quad (17)$$

which yields a simpler propagating equation

$$|\Psi_p(t+\Delta)\rangle=e^{-(i/\hbar)H\Delta}[|\Psi_p(t)\rangle+(1-e^{-V_p\Delta/\hbar})|\Psi_r(t)\rangle]. \quad (18)$$

Equation (18) is more accurate than an earlier propagator used in previous applications

$$|\tilde{\Psi}_p(t+\Delta)\rangle=e^{-(i/\hbar)H\Delta}|\tilde{\Psi}_p(t)\rangle+\frac{\Delta}{\hbar}V_p|\Psi_r(t+\Delta)\rangle, \quad (19)$$

where $\tilde{\Psi}_p(t)=\Psi_p(t)+(\Delta/2\hbar)V_p\Psi_r(t)$.

In this TD approach, we need to store the calculated source term $\xi_p(t)=V_p\Psi_r(t)$ as in Eq. (19) or $(1-e^{-V_p\Delta/\hbar})\Psi_r(t)$ in Eq. (18). We also need to represent the $\xi_p(t)$ in the product Jacobi coordinates to facilitate the propagation. This will require a coordinate transformation at every time step for which $\xi_p(t)$ is nonzero.

An alternative approach is to use the time-independent version of Eq. (2),

$$\begin{aligned}E|\psi_r(E)\rangle&=H|\psi_r(E)\rangle-i\sum_p V_p|\psi_r(E)\rangle,\\ E|\psi_p(E)\rangle&=H|\psi_p(E)\rangle+iV_p|\psi_r(E)\rangle,\end{aligned} \quad (20)$$

and solve the TI product wave function $\psi_p(E)$ by

$$|\psi_p(E)\rangle=iG^+(E)V_p|\psi_r(E)\rangle=\frac{1}{\hbar}\int_0^\infty dt e^{(i/\hbar)Et}e^{-(i/\hbar)Ht}V_p|\psi_r(E)\rangle=\frac{1}{\hbar}\int_0^\infty dt e^{(i/\hbar)Et}|\xi_p(t,E)\rangle \quad (21)$$

where

$$|\xi_p(t,E)\rangle=e^{-(i/\hbar)Ht}V_p|\psi_r(E)\rangle. \quad (22)$$

In Eq. (21), the wave function $\psi_p(E)$ is obtained by propagating the energy-dependent wave packet $\xi_p(E)=V_p\psi_r(E)$ and performing the Fourier transform afterwards for each desired energy. The wave function $\psi_r(E)$ is obtained by Fourier transforming the time-dependent wave function $\psi_r(t)$, which is obtained by wave packet propagation described previously. This approach is attractive if dynamics at a limited

number of energies are desired because in this case, we only need to store the source term $\xi_p(E)=V_p\psi_r(E)$ for the number of energies needed.

After the wave packet is fully developed in the inelastic region of the specific product arrangement with proper absorbing boundary conditions, one can straightforwardly perform the final state analysis in the asymptotic region (R' large) to obtain the energy-dependent S matrix elements or reaction probabilities by Fourier transforming the TD wave function $\Psi_p(t)$ to $\Psi_p(E)$ at large asymptotic distance

$$\psi_p(E) \overset{R'\to\infty}{\to} \sqrt{\frac{\mu_p}{2\pi\hbar^2}}\left[\sum_m S_{pm,ri}\frac{e^{ik_mR'}}{\sqrt{k_m}}|\eta_{pm}\rangle\right], \qquad (23)$$

where μ_p is the reduced translational mass and η_{pm} the internal channel function in the pth product arrangement. If any long-range elastic potential is present such as the centrifugal potential, one needs to replace the plane wave function $e^{ik_mR'}$ by the outgoing Hankel or other appropriate radial function. Alternatively, if only square of the S matrix element or reaction probability is required, one can avoid specifying the specific form of the radial function and instead evaluate the flux to obtain converged reaction probability at a relatively shorter radial distance.[18] For transformation of Jacobi coordinates between reactant and product arrangements, the reader is referred to Ref. 9 for details.

III. RESULTS

We performed a time-dependent wave packet calculation to obtain the state-to-state transition probabilities for the reaction $Cl+H_2\to HCl$ on the G3 PES. The wave packet calculation is carried out by using the RPD method of Ref. 8 to separate the full wave function into reactant and product components. The numerical calculation is done for zero total angular momentum ($J=0$) with the initial reactant H_2 at ground rovibrational state ($v=j=0$) only. The $Cl+H_2$ reaction is slightly endothermic (by about 1 kcal/mol) and with a classical barrier of almost 6 kcal/mol.[15] In the present RPD calculation, the absorbing potential V_p is defined in terms of the product translational coordinate and ranged from 5.6 to 8.5 bohr. Figure 1 shows the energy dependence of the reaction probabilities for producing specific vibrational states of the product HCl. The total energy in the Fig. 1 includes both the initial vibrational energy and the translation energy. These results are in good agreement with a recent time-independent variational scattering calculation for the $Cl+H_2$ reaction by Alagia *et al.* (see Fig. 9 of Ref. 19).

Figure 2 shows specific rotational state distribution of the product HCl corresponding to the $v'=0$ vibrational state at several scattering energies. At the total scattering energy of 0.48 eV, the rotational distribution is peaked at $j'=4$ as shown in Fig. 2. As the scattering energy increases to 0.55 and to 0.71 eV, the peak of the probability distribution shifts to $j'=5$ and $j'=6$, respectively. This is typical. As the scattering energy increases, the maximum rotation distribution shifts to higher values of j' because more rotational states are populated. However, as the energy further increases to 0.9 eV, the maximum of the rotation distribution actually *decreases* to $j'=4$ again. In addition there is a second small peak formed around $j'=15$ at 0.9 eV, making it a bimodal-like distribution of rotational states. From Fig. 1 it is clear that at 0.9 eV, the reaction probability for the ground product vibrational state $v'=0$ has declined significantly accompanied by a corresponding increase in probability for the excited vibrational state $v'=1$. Thus the decrease in rotation-specific reaction probability at high energy has to be compensated by an increase in reaction probability to the vibrationally excited states.

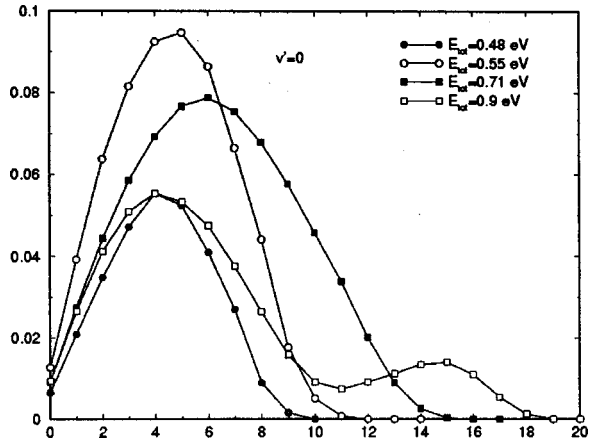

FIG. 2. Rotational state distribution for the reaction $Cl+H_2(00)\to ClH(v'=0,j')$ at total scattering energy of 0.48, 0.55, 0.71, and 0.9 eV.

Figure 3 shows the rotational state distribution for the vibrationally excited state $v'=1$ at a total energy of 0.9 eV. It is interesting to note in Fig. 3 that the rotational state distribution also has two maxima: a major one at $j'=2-3$ and a minor one at $j'=10$. This bimodal distribution at high energy at $v'=1$ is similar to that for the ground vibrational state $v'=0$ in Fig. 2 except that the second peak is shifted to lower j' value for the excited vibrational state. At present, we do not have a clear explanation for the bimodal distribution at high scattering energies.

In Fig. 4, we show the energy dependency of reaction probabilities for producing the specific rotational states– $P_{j'}(E)=\Sigma_{v'}P_{v'j'}(E)$, where contributions from different

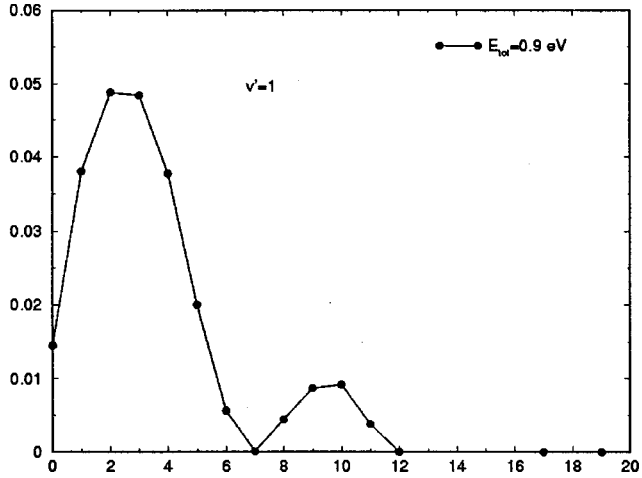

FIG. 3. Rotational state distribution for the reaction $Cl+H_2(00)\to HCl(v'=1,j')$ at the total energy of 0.9 eV.

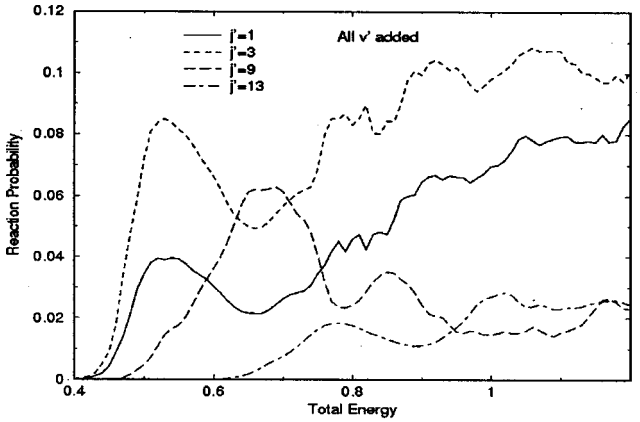

FIG. 4. Energy dependence of the rotation-specific reaction probability for $Cl+H_2(00)\rightarrow HCl(j')+H$ where the product vibrational states v' have been summed over.

vibrational states of the product are summed over. It is shown that the $j'=3$ state is more preferable than the $j'=0$ state, as is consistent with the result of Fig. 2. A similar energy-dependent result is shown in Fig. 5 for several rotational states of the product at ground vibrational state $(v'=0)$.

IV. DISCUSSIONS AND PROSPECTIVES

In this paper we presented a numerical application of the RPD method to the three-dimensional state-to-state calculation for $Cl+H_2$ reaction on the G3 potential energy surface. Our result demonstrates that accurate state-to-state reactive scattering results can be obtained from a time-dependent wave packet calculation using the RPD approach to partition the wave function into reactant and product regions. Because of the generality of the RPD approach and the flexibility in choosing the form and location of the ''absorbing'' potential V_p in the application of RPD method, further investigation on the optimal use of the absorbing potential is needed to improve the efficiency of the RPD method. A recent work by Althorpe demonstrated that by applying a ''reflecting'' potential near the entrance channel in the RPD approach can significantly improve the numerical efficiency of the wave packet calculation by reducing the number of product basis functions or quadrature points that are required to represent the product component wave function Ψ_p.[14] The efficient calculation of the differential cross section for the $H=H_2$ in Ref. 14 and the current demonstration of the RPD approach for the $Cl+H_2$ reaction are making it possible for efficient time-dependent wave packet calculation of state-to-state differential cross sections for more complex reaction systems.

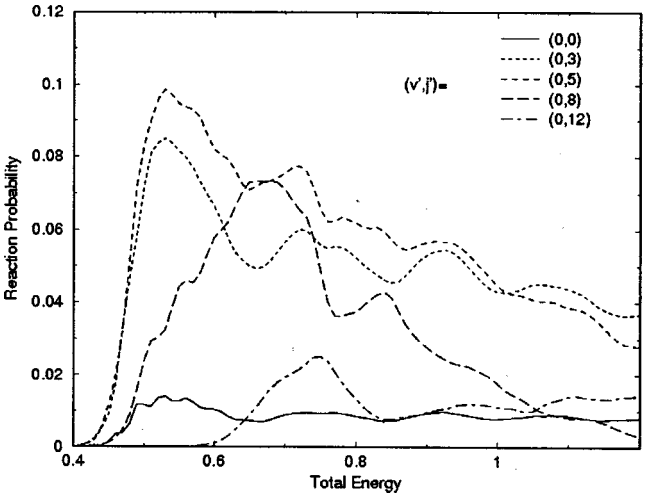

FIG. 5. Energy dependence of the rovibration-specific reaction probability for $Cl+H_2(00)\rightarrow HCl(v',j')+H$.

ACKNOWLEDGMENTS

This work is supported by the National Natural Science Foundation of China under Grant No.19774038 and No.19874040, Shandong Province Science Foundation under Grant No. 99A04. One of the authors (J.Z.H.Z.) acknowledges the financial support from National Science Foundation of U.S.A. under Grant No. CHE-0072183 and Petroleum Research Fund administered by the American Chemical Society. J.Z.H.Z. also acknowledges helpful discussions with Professor Dong H. Zhang on propagating the RPD equations.

[1] J. Z. H. Zhang, J. Dai, and W. Zhu, J. Phys. Chem. A **101**, 2746 (1997).
[2] D. H. Zhang, M. A. Collins, and S. Y. Lee, Science **290**, 889 (2000).
[3] M. L. Wang, Y. Li, J. Z. H. Zhang, and D. H. Zhang, J. Chem. Phys. **13**, 1802 (2000).
[4] M. L. Wang, Y. M. Li, and J. Z. H. Zhang, J. Phys. Chem. A **105**, 2530 (2001).
[5] F. Huarte-Larranaga and U. Manthe, J. Chem. Phys. **113**, 5115 (2000).
[6] R. S. Judson, D. J. Kouri, D. Neuhauser, and M. Baer, Phys. Rev. A **42**, 351 (1990).
[7] F. Gogtas, G. G. Balint-Kurti, and A. R. Offer, J. Chem. Phys. **104**, 7927 (1996).
[8] T. Peng and J. Z. H. Zhang, J. Chem. Phys. **105**, 6072 (1996).
[9] W. Zhu, T. Peng, and J. H. Z. Zhang, J. Chem. Phys. **106**, 1742 (1997).
[10] J. Dai and J. H. Z. Zhang, J. Chem. Soc., Faraday Trans. (in press).
[11] D. J. Kouri, D. K. Hoffman, T. Peng, and J. Z. H. Zhang, Chem. Phys. Lett. **262**, 519 (1996).
[12] S. C. Althorpe, D. J. Kouri, and D. K. Hoffman, J. Chem. Phys. **107**, 7816 (1997).
[13] S. C. Althorpe, D. J. Kouri, and D. K. Hoffman, J. Phys. Chem. A **102**, 9494 (1998).
[14] S. C. Althorpe, J. Chem. Phys. **114**, 1601 (2001).
[15] T. C. Allison, G. C. Lynch, D. G. Truhlar, and M. S. Gordon, J. Phys. Chem. **100**, 13575 (1996).
[16] D. H. Zhang and J. Z. H. Zhang, J. Chem. Phys. **101**, 1146 (1994).
[17] J. A. Fleck, J. R. Morris, Jr., and M. D. Feit, Appl. Phys. **10**, 129 (1976).
[18] J. Dai and J. Z. H. Zhang, J. Phys. Chem. **100**, 6898 (1996).
[19] M. Alagia, N. Balucani, L. Cartechini, P. Casavecchia, G. G. Volpi, F. J. Aoiz, L. Banares, T. C. Allison, S. L. Mielke, and D. G. Truhlar, Phys. Chem. Chem. Phys. **2**, 599 (2000).